Local, cell-nonautonomous feedback regulation of myosin dynamics patterns transitions in cell behavior: a role for tension and geometry?

Surat Saravanan, C. Meghana, and Maithreyi Narasimha
Department of Biological Sciences, Tata Institute of Fundamental Research, Colaba, Mumbai 400005, India

ABSTRACT **How robust patterns of tissue dynamics emerge from heterogeneities, stochasticities, and asynchronies in cell behavior is an outstanding question in morphogenesis. A clear understanding of this requires examining the influence of the behavior of single cells on tissue patterning. Here we develop single-cell manipulation strategies to uncover the origin of patterned cell behavior in the amnioserosa during *Drosophila* dorsal closure. We show that the formation and dissolution of contractile, medial actomyosin networks previously shown to underlie pulsed apical constrictions in the amnioserosa are apparently asynchronous in adjacent cells. We demonstrate for the first time that mechanical stresses and Rho1 GTPase control myosin dynamics qualitatively and quantitatively, in amplitude and direction, both cell autonomously and nonautonomously. We then demonstrate that interfering with myosin-dependent contractility in single cells also influences pulsed constrictions cell nonautonomously. Our results suggest that signals and stresses can feedback regulate the amplitude and spatial propagation of pulsed constrictions through their influence on tension and geometry. We establish the relevance of these findings to native closure by showing that cell delamination represents a locally patterned and collective transition from pulsed to unpulsed constriction that also relies on the nonautonomous feedback control of myosin dynamics.**

Monitoring Editor
Alex Mogilner
University of California, Davis

Received: Dec 12, 2012
Revised: May 28, 2013
Accepted: May 29, 2013

INTRODUCTION

Cell-shape changes, cell rearrangements, and cell movements power tissue morphogenesis, individually or in combination (Lecuit and Le Goff, 2007). The complex geometries that characterize the final form of tissues necessitate heterogeneities in cell behavior. How heterogeneities are generated and coordinated and how they influence the spatial patterning of tissues is an unresolved problem in morphogenesis. An understanding of this requires the ability to manipulate and perturb single cells. The complex morphogenesis of the amnioserosa during dorsal closure provides an attractive model in which these questions can be addressed.

Localized cell-shape changes, notably apical constriction, can accomplish bending, internalization, contraction, or elongation of epithelial sheets during morphogenesis (Sawyer *et al.*, 2009). Contraction of the amnioserosa (AS), the major force provider for *Drosophila* dorsal closure (Kiehart *et al.*, 2000; Narasimha and Brown, 2004), is also driven by apical constriction. Recent studies show that apical constriction in some tissues is not continuous but is interrupted by periods of relaxation or stabilization to produce cycles with characteristic amplitudes and frequencies (Martin *et al.*, 2009; Blanchard *et al.*, 2010; He *et al.*, 2010). In the amnioserosa, apical constriction is pulsed in the early phase (phase I; cycles of constriction and relaxation) and unpulsed later in dorsal closure (phase II) when the cells proceed to constrict without intervening relaxation phases (Gorfinkiel *et al.*, 2009; Solon *et al.*, 2009). Rapid constriction without intervening relaxation is also a feature of cell delamination (Meghana *et al.*, 2011), a seemingly stochastic cell behavior observed in both phase I and phase II. What drives the transition from pulsed to unpulsed constriction is unclear.

Pulsed apical constrictions correlate with the dynamics of an actomyosin complex that is medial (localized under the apical surface)

This article was published online ahead of print in MBoC in Press (http://www.molbiolcell.org/cgi/doi/10.1091/mbc.E12-12-0868) on June 5, 2013.

Address correspondence to: Maithreyi Narasimha (maithreyi@tifr.res.in).

Abbreviations used: AS, amnioserosa; CI, cell constriction index; DC, delaminating cell; DiNe, distant neighbor; GFP, green fluorescent protein; LC, labeled cell; LPC, laser-perturbed cell; MLC, myosin light chain; NeNe, nearest neighbor; pMLC, phosphorylated myosin light chain; Wt, wild type; YFP, yellow fluorescent protein.

rather than lateral (the stable pool associated with the circumapical cortex) and is localized apically except in the case of the follicle epithelium, where it is basal (Martin *et al.*, 2009; Blanchard *et al.*, 2010; He *et al.*, 2010). Several issues remain largely unresolved, including 1) the molecular composition of this complex, 2) the regulators of its dynamics, 3) the nature and origin of cues that drive it, and 4) its utility for a morphogenetically active tissue. Unlike the contraction–stabilization cycles that characterize apical constriction during *Drosophila* ventral furrow invagination, the pulses in the amnioserosa are characterized by contraction–relaxation cycles accompanied by area and shape fluctuations about a mean (Martin *et al.*, 2009; Solon *et al.*, 2009). In addition, unlike constrictions in the follicle epithelium, in which pulsed constrictions are basal and achieve tissue elongation (He *et al.*, 2010), in the amnioserosa they mediate tissue contraction. Each tissue hitherto studied exhibits a characteristic pulse periodicity, the basis of which is also largely unclear.

A diverse set of molecules influence pulsed constriction. The mesodermal transcription factors Twist and Snail differentially influence the contraction and stabilization phases of pulsed constriction during ventral furrow invagination, presumably through their distinct targets (Martin *et al.*, 2009). Adhesion molecules at cell–cell junctions have been suggested to serve as membrane tethers or as cues that guide medial myosin complexes and facilitate apical membrane constriction (Dawes-Hoang *et al.*, 2005; Martin *et al.*, 2010; Rauzi *et al.*, 2010). Integrin-based adhesions influence both amplitude and frequency of basal pulsed constrictions in the follicle epithelium (He *et al.*, 2010). Mutations in the polarity regulators Par-6 and Bazooka influence pulse amplitudes in the amnioserosa (David *et al.*, 2010). One study demonstrated that the pulse amplitude of amnioserosa cells is influenced by the leading edge cells of the epidermis, the actin cable that forms at its dorsal edge acting like a ratchet. Abolition of tension in the leading edge was shown to lead to a failure of dampening of oscillations and phase II (Solon *et al.*, 2009). Another study, however, argued that pulsed constrictions are solely influenced by the genetic constitution of the amnioserosa (Blanchard *et al.*, 2010). As evidence for this, the authors showed that inactivation of the Rho1 GTPase only in the amnioserosa was sufficient to reduce the amplitude of pulsed constrictions and that perturbations influencing tension in the leading edge failed to influence it. What signals regulate these pulsed constrictions in space and time and what purpose they serve for the tissue are largely unclear.

In the work we describe here, we develop biophysical and genetic perturbation strategies restricted to single cells in the amnioserosa during phase I to investigate 1) whether the transition from pulsed to unpulsed constrictions is regulated cell autonomously or is influenced by cues from the surrounding cells, 2) whether this relies on mechanical cues or chemical cues, and 3) the influence of single-cell perturbations on the organization and dynamics of the actomyosin cytoskeleton and the spatial patterning of the tissue. We use these perturbations singly and in combination (Meghana *et al.*, 2011) and demonstrate that mechanical stresses (delivered by laser ablation) and chemical signals (Rho1 GTPase) can locally and nonautonomously modulate pulse amplitudes, cause cytoskeletal reorganization and polarization, and induce rapid and reversible transitions from pulsed to unpulsed cell behavior. We further demonstrate that cell delamination occurring during native closure is characterized by a similar transition that is collective, locally patterned, and nonautonomously regulated. We suggest that the similarities in the effects of both perturbations may lie in their similar effects on tension and geometry. We discuss the implications of our findings on the spatial propagation and utility of pulsed behavior for active epithelia.

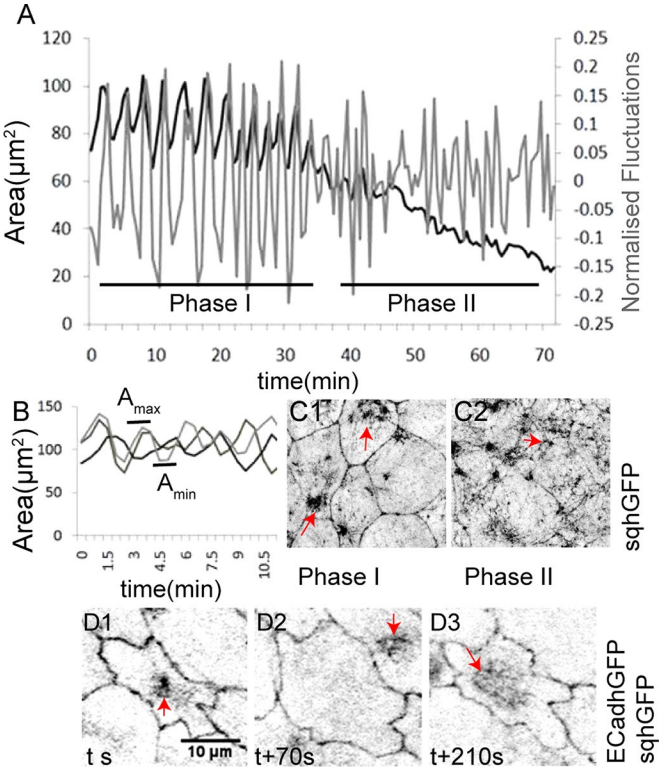

FIGURE 1: Membrane and myosin dynamics accompanying pulsed apical constrictions in the amnioserosa. (A) A representative curve of the apical area dynamics (black) and normalized fluctuations (gray) of a single AS cell during native closure. Asynchrony of *A*max and *A*min (B) and sqhGFP pulses (D1–D3, red arrows) in three adjacent cells from one embryo. (C1, C2) Myosin (sqhGFP, red arrows) reorganization accompanying the transition from phase I to phase II.

RESULTS

Pulsed apical constrictions in adjacent cells in the amnioserosa are apparently asynchronous

A feature of phase I of amnioserosa morphogenesis is pulsed apical constriction, characterized by pulsed shape and area changes that exhibit apparent asynchrony in neighboring cells (Figure 1, A and B; $n = 12$ cells from three embryos). This is followed (phase II) by collective pulse dampening, leading to rapid apical area reduction (Figure 1A; Blanchard *et al.*, 2010). The cycles of formation and dissolution of medial myosin (visualized using a green fluorescent protein [GFP]-tagged version of the *Drosophila* regulatory myosin light chain [MLC], sqhGFP) also exhibit apparent asynchrony in adjacent cells in phase I (Figure 1, D1–D3). Within each cell, medial, contractile myosin foci that form and dissolve correlate with its area oscillations in the early phase, whereas cortical enrichment and apical myosin meshworks are associated with the collective, rapid reduction in cell area in the late phase (Figure 1, C1 and C2, and Supplemental Movie S1a; Blanchard *et al.*, 2010).

Myosin dynamics influences pulsed apical constrictions autonomously and nonautonomously

To establish a causal role for the observed myosin dynamics in pulsed constriction, we expressed a mutant myosin that fails to bind actin in the entire amnioserosa. This myosin (UAS mYFP myosin II^{DN}, hereafter called myo II^{DN}; Dawes-Hoang *et al.*, 2005) is contraction defective, since its motor domain is replaced by yellow fluorescent protein (YFP). myo II^{DN} was shown to be defective in its

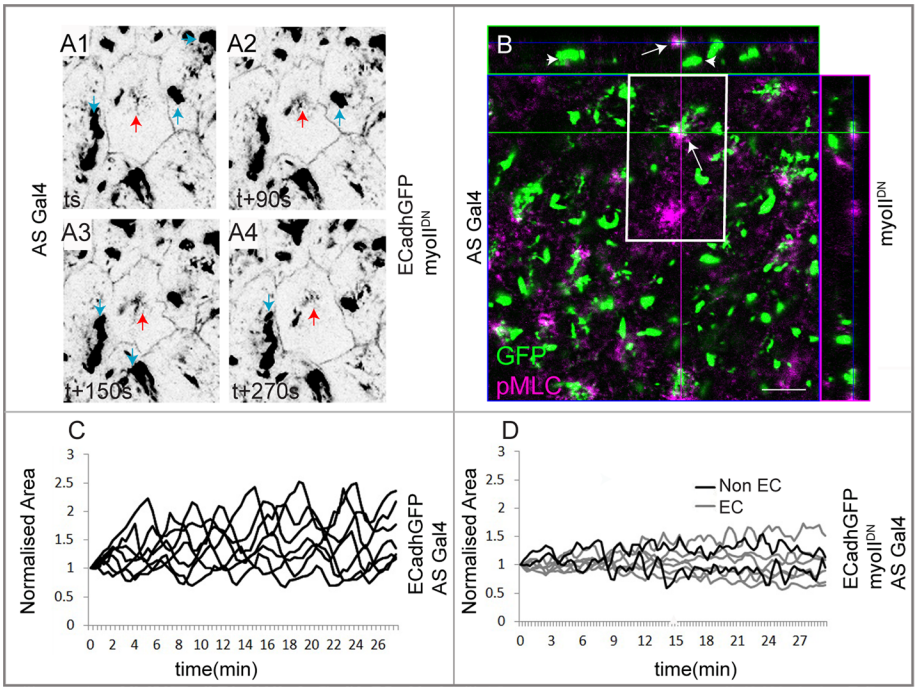

FIGURE 2: The influence of myosin contractility and dynamics on pulsed apical constrictions in the amnioserosa. (A1–A4) AS cells expressing E-cadherin–GFP and myoII^{DN}, revealing two medial pools of YFP: a larger, immotile pool (blue arrows) and a smaller, motile pool (red arrows). Partial colocalization of YFP (green) and pMLC (purple, arrows in B) is seen in the smaller, apically localized motile pool but not in the larger, more widely distributed immotile pool (arrowheads in B). The central image in B represents an apical *XY* section; the panels on top and to the right represent orthogonal *XZ* and *YZ* sections. (C) Normalized area (visualized with ECadhGFP) of control AS cells carrying ASGal4 but not myoII^{DN} ($n = 7$ cells from three embryos). (D) Normalized area dynamics of AS cells expressing (EC, gray; 5 cell traces of a total of 11 examined from three embryos) or not expressing (Non EC, black; two cell traces of a total of five from three embryos) myoII^{DN} driven by the patchy ASGal4. Scale bar, 10 μm. See also Supplemental Figure S1.

localization to some but not all myosin pools in cells of the invaginating mesoderm during *Drosophila* gastrulation (Dawes-Hoang *et al.*, 2005). We therefore first examined the influence of the myo II^{DN} on the organization of contractile actomyosin complexes in amnioserosa cells using an antibody to the phosphorylated form of MLC (pMLC). In sqhGFP embryos that are otherwise wild type, GFP and pMLC colocalize within medial myosin foci in the amnioserosa, thus identifying the contractile, motile pool. Overall they are present in largely overlapping patterns (Supplemental Figure S1, C1–C3). In contrast, two pools of myo II^{DN} could be identified in expressing cells in phase I: a large, discrete, immotile pool that was not labeled with pMLC and a smaller, more diffuse pool that partially colocalized with pMLC (Figure 2B). The latter was also weakly motile (Figure 2, A1–A4, and Supplemental Movie S1b) and exhibited some contraction and dispersion but no coalescence or dissolution (Supplemental Movie S1, a and b). Its expression in amnioserosa cells resulted in a reduction in the amplitude of area oscillations (visualized by E-cadherin GFP) not only in the cells expressing it, but also in the nonexpressing cells (resulting from patchy Gal4 expression). In contrast, cells from embryos carrying Gal4 but not myo II^{DN} exhibited wild-type oscillatory behavior (Figure 2, C and D, and Supplemental Figure S1, A and B). These results establish that motile myosin complexes are necessary across the amnioserosa for pulsed cell behavior.

The existence of two distinct phases, the asynchronous dynamics between adjacent cells, the heterogeneities in cell behavior within phase I (pulsed constriction and cell delamination) during native closure, and the cell-nonautonomous effects of myo II^{DN} prompted us to investigate whether mechanical cues or tension can pattern and propagate transitions in pulsed cell behavior. For this, we used mechanical perturbation strategies for single amnioserosa cells.

Single-cell mechanical perturbations influence pulsed constrictions both autonomously and nonautonomously

We previously developed a strategy to perturb cell mechanics (release cellular prestress) in single cells using nanoscale cytoplasmic laser ablation (hereafter called LPC for laser-perturbed cell; Meghana *et al.*, 2011). In late phase I AS cells, such a perturbation results in dynamic changes in cell geometry characterized by cell expansion (a manifestation of the release of cellular prestress), followed by cell constriction and the eventual delamination/extrusion of the LPC. We also established the dynamic and reciprocal changes in geometry in the nearest neighbors (NeNe) of the LPC. Cell expansion alters cell morphology of the nearest neighbors such that they become progressively shorter along the radial axis and stretched along the azimuthal axis. The constriction that follows is associated with stretch and shortening in the opposite axes, radial and azimuthal respectively, of the nearest neighbors (Figure 3, A1–A4; Meghana *et al.*, 2011). This enables us to achieve dynamic alterations in tension and geometry in the LPC (release of prestress) and in the nearest neighbors. We used this to ask whether mechanical or topological cues might influence pulsed apical constrictions.

We perturbed AS cells in phase I of dorsal closure and followed area dynamics. We divide the response to the perturbation into four time regimes with respect to the changes in the LPC: preablation (A), expansion (B), constriction (C), and postextrusion (D). As observed earlier (Meghana *et al.*, 2011), pulses in the LPC evident in the preablation phase are dampened as the cell begins to expand and continue to remain dampened throughout the constriction phase until the cell is extruded. Surprisingly, pulses were also dampened in its nearest neighbors in the expansion and early constriction phases ($n = 5$ for LPC and 10 for NeNe). Distant neighbors (DiNe, $n = 8$ from five embryos), however, are unaffected (Figure 3B). Further, whereas the dampening persists through phases B and C in the perturbed cell, it is partially lifted in the nearest neighbors as the perturbed cell is extruded. This partial recovery of pulsed constrictions begins in the late constriction phase (phase C; ~557 ± 28 s after ablation), before cell extrusion (786.2 ± 31 s after ablation; Figure 3B and Supplemental Figure S2, A1–A4) and is evident in the significant differences in normalized pulse amplitudes (before ablation [0.3 ± 0.02], during the expansion–contraction phases [pulses abolished], and upon extrusion [0.16 ± 0.01; $p < 0.0001$]) in the nearest neighbors. These results suggest that changes in tension and geometry induced by mechanical perturbations can influence pulsed cell behavior dynamically, reversibly, locally, and cell nonautonomously.

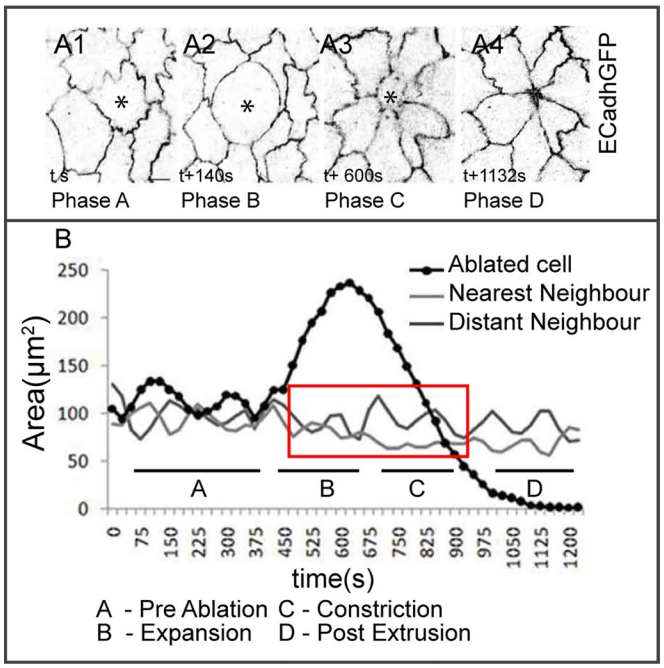

FIGURE 3: Autonomous and nonautonomous membrane dynamics in response to laser perturbation. Representative membrane (A1–A4) and apical area dynamics (B) of a laser-perturbed cell (asterisk in A1–A4, black in B), its NeNe (light gray in B), and DiNe (dark gray in B) highlighting distinct phases (A, preablation; B, expansion; C, constriction; and D, postextrusion) of the response. Red box in B shows the dampened phase. See Supplemental Figure S2 for further examples. $n = 5$ for LPC, 10 for NeNe, and 8 for DiNe from five embryos. Scale bar, 10 μm.

To rule out the possibility that the changes we observed were a unique feature of laser ablation and establish that they resulted from changes in tension and geometry, we altered tension and geometry in single cells through genetic perturbations of the Rho1 GTPase.

Single-cell genetic perturbations reveal nonautonomous influences of Rho1

To enable single-cell genetic perturbations, we screened a collection of Gal4 lines for their ability to drive expression in amnioserosa cell subsets (M.N., unpublished results) and identified one (engrailedGal4 [enGal4]; see *Materials and Methods*) that drives expression in single cells in the amnioserosa in addition to stripes in the epidermis. We used this in conjunction with UAS actin5CGFP to label the perturbed cell (LC) and assay its influence on pulsed constrictions in the LC and its nearest and distant neighbors (Figure 4A1). We examined the effect of perturbing the Rho1 GTPase for the following reasons. First, Rho1 was shown to affect pulsed constrictions in the amnioserosa in a tissue autonomous manner (Blanchard *et al.*, 2010). Second, Rho1 is a potent regulator of cell morphology and mechanics through its effects on the actomyosin and microtubule cytoskeletons, as well as on cell adhesion (Jaffe and Hall, 2005). Indeed both effects were also observed in Rho1 perturbations induced in fly tissues (Bloor and Kiehart, 2002). Third, its ability to cycle between active and inactive states by regulated nucleotide binding make it an attractive candidate for enabling transitions in cell behavior.

To explore the influence of Rho1 on pulsed constrictions in the amnioserosa, we used dominant-negative (RhoN19) and constitutively active (RhoV14) UAS transgenes to down-regulate or activate Rho1, respectively (Figure 4 and Supplemental Figures S3 and S4; see *Materials and Methods*). The additional presence of E-cadherin–GFP enabled the visualization of the behavior of the apical surface of the genetically perturbed cell (LC), as well as its nearest and distant neighbors, and the measurement of area dynamics and pulse amplitudes. The pulse dynamics of marked unperturbed cells (Wt) is shown in Figure 4, A1–A3, and Supplemental Figures S3, A1–A3, and S4, A1–A3 ($n = 3$ for LC, 8 for NeNe, and 6 for DiNe from three embryos). Down-regulating Rho resulted in marked and progressive expansion of the expressing cell (Figure 4B1 and Supplemental Movie S2). This also resulted in changes in cell geometry in the nearest neighbors, characterized by the progressive shortening of the nearest neighbors along the axis perpendicular to the interface with the perturbed cell (radial) and stretching along the axis parallel to it (azimuthal). Further, the analysis of the area dynamics of the RhoN19 LC revealed the abolition of the two phases of apical constriction, as well as of the oscillations in area that characterize phase I (Figure 4B2 and Supplemental Figure S3, B1–B3). Unexpectedly, pulsations were also dampened in its nearest neighbors (Figures 4B3 and Supplemental Figure S3, B1–B3; $n = 3$ for LC, 10 for NeNe, and 5 for DiNe from three embryos). We believe that this dampening cannot result from Rho down-regulation in epidermal stripes, as distant neighbors show pulse amplitudes that are comparable to wild type.

In contrast, its constitutive activation in single cells resulted in precocious and stable apical constriction that did not culminate in delamination (Figure 4C1). This resulted in the stable stretching and shortening of the nearest neighbors along the radial and azimuthal axes, respectively. The constriction caused dampened pulsations in the perturbed cell and also in the nearest and distant neighbors (Figure 4, C2–C3, Supplemental Figure S4, A1–A3 and B1–B3, and Supplemental Movie S3; $n = 3$ for LC, 10 for NeNe, and 5 DiNe from three embryos). Thus, whereas down-regulating and activating Rho1 have opposite effects on apical surface area and local cell geometries, both abolish the phases and pulses characteristic of wild-type cell behavior, with RhoN19 affecting it locally and cell nonautonomously (in the nearest but not distant neighbors) and RhoV14 additionally showing long-range effects (in the nearest and distant neighbors). This suggests that cycling of the Rho1 GTPase is essential to maintain pulsed cell behavior. Importantly, it uncovers cell-nonautonomous influences of Rho1 on cell geometry and pulsed behavior not previously demonstrated. Further, the similarities in the influence of dynamic tension and geometry induced by laser ablation and the relatively stable geometries induced by Rho perturbations on pulsed constrictions suggest that similar downstream mechanisms might underlie both.

One mechanism by which locking Rho1 into active or inactive states might influence pulsed behavior is through its effect on cytoskeletal dynamics. Indeed, work in other systems (Watanabe *et al.*, 1999; Bershadsky *et al.*, 2006) revealed the existence of two pathways that diverge downstream of RhoA and differ in their deployment of effectors and the subsequent mode of cytoskeletal reorganization. The major target of one of these pathways, involving the Rho kinase ROCK, is myosin. Given that myosin dynamics underlies pulsed behavior, we examined the possibility that changes in myosin dynamics and organization underlie the influence of both mechanical and genetic perturbations.

Single-cell mechanical and genetic perturbations are accompanied by changes in medial myosin dynamics in nearest neighbors

To investigate the influence of dynamic geometries and interfacial tensions induced by both kinds of perturbations on pulsed

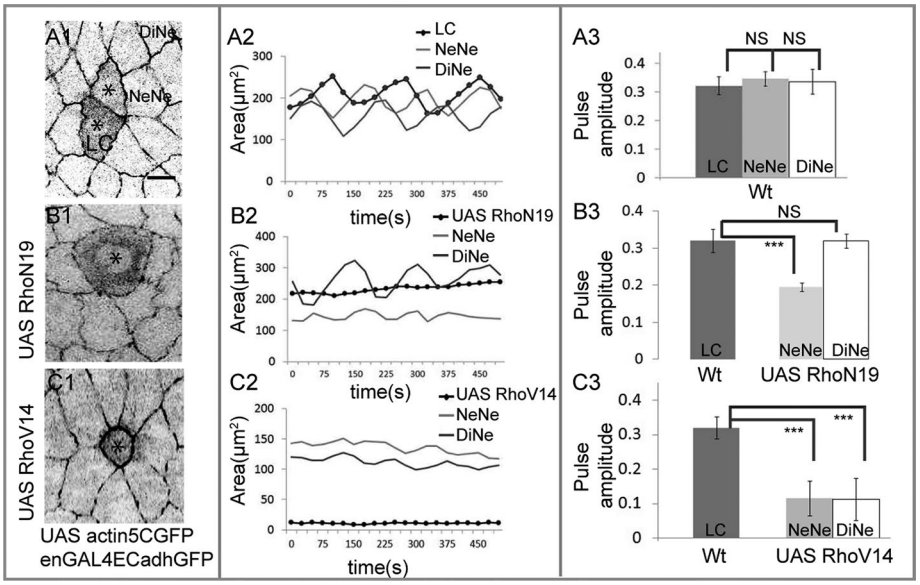

FIGURE 4: The Rho1 GTPase influences pulsed apical membrane dynamics autonomously and nonautonomously. The behavior of cohorts of wild-type cells and their neighbors (A) compared with cohorts of single cells expressing dominant-negative (B) or constitutively active (C) Rho. Left (A1, B1, C1), single snapshots from time-lapse confocal images depicting changes in geometry associated with expression of actin GFP alone (A1) or in combination with dominant negative (B1) or constitutively active (C1) Rho in single cells (asterisk in A1, B1, C1) and in their NeNe and DiNe. Middle (A2, B2, C2), area dynamics respectively of one cohort each associated with a single cell expressing UAS Actin5CGFP alone (A2) or in combination with UAS RhoN19 (B2) or UAS RhoV14 (C2). Each cohort is represented by one labeled/perturbed cell (black curves in A2, B2, C2) and one NeNe and one DiNe (light and dark gray curves, respectively, in A2, B2, C2). Right (A3, B3, C3), pulse amplitudes (mean ± SD) of the NeNe (light gray bars) and DiNe (white bars) of cells expressing UAS RhoN19 (B3) or UAS RhoV14 (C3) in comparison with the amplitude of unperturbed labeled cells (LC, dark gray bars), which are indistinguishable from their NeNe and DiNe (A3). See Supplemental Figures S3 and S4 for supporting data. A3: $n = 3$ for LC, 8 for NeNe, and 6 for DiNe from three embryos. B3: $n = 3$ for LC, 10 for NeNe, and 5 for DiNe from three embryos. C3: $n = 3$ for LC, 10 for NeNe, and 5 for DiNe from three embryos. ***$p < 0.001$. Scale bar, 10 μm.

constrictions, we performed a high-resolution analysis of the spatiotemporal dynamics of medial myosin accompanying mechanical and genetic perturbation.

All myosin complexes are irreversibly lost in the laser-perturbed cell, presumably accounting for its inability to pulse. In the nearest neighbors, on the other hand, motile medial myosin complexes that characterize the preablation phase were replaced by myosin meshworks formed from directional streaming toward the perturbed cell in the expansion phase (Figure 5, A1–A2). In the constriction phase, medial motile complexes reappeared in the nearest neighbors but were collectively directed toward the perturbed constricting cell (Figure 5A3). Remarkably, after cell extrusion, these became randomly directed, as in the preablation phase (Figure 5A4 and Supplemental Movie S4). These observations uncover the remarkable power of changes in tension and geometry to direct cytoskeletal organization not only in the LPC, but also in the nearest neighbors, and suggest that changes in cytoskeletal organization (meshwork in the expansion phase and directed motility in the contraction phase) might underlie changes in pulsed behavior.

We next examined the dynamics of myosin accompanying single-cell perturbations of Rho1. In the RhoN19 LC, no contractile foci of myosin were visible (Figures 5, B1–B3). Although motile myosin complexes were found in the nearest neighbors, they appeared more diffuse and less dynamic compared with distant neighbors and were often found to traverse the cell along the stretched axis of the cell, toward the shortened interfaces (Figure 5, B1–B3, and Supplemental Movie S5). To delineate the differences in myosin behavior in the nearest- and distant-neighbor cells, we analyzed deviations in myosin intensity across multiple cohorts of nearest neighbors and in multiple individual nearest neighbors across time (Table 1; see *Materials and Methods*). We used the former to infer spatial (a)synchrony/collectivity of myosin reorganization among the nearest neighbors ("synchrony"), whereas the latter is suggestive of the temporal dynamics of medial myosin complexes in each nearest neighbor ("dynamics"). Myosin organization seemed more collective and less dynamic in the nearest neighbors around each LC measured ($n = 16$ cells from four embryos), as inferred from the decreased deviations in myosin intensity around the mean, in contrast to the distant neighbors ($n = 10$ from four embryos; Table 1), whose values were comparable to those observed in an unperturbed cohort. The observed changes might contribute to the dampening in the membrane response of the nearest neighbors (Figure 3B3).

In contrast, constitutive activation of Rho1 resulted in the stable accumulation of myosin in the perturbed cell. In its nearest neighbors, myosin exhibited directed movement toward the constricted cell (Figure 5, C1–C3, and Supplemental Movie S6). To investigate the origin of dampening in the membrane response of nearest neighbors and distant neighbors upon activating Rho (Figure 4C3), despite the presence of motile myosin complexes, we quantified the time taken for each myosin cycle, specifically for the formation of the medial myosin complex and its subsequent dissolution. The times for both were elevated in this genetic background in nearest- and distant-neighbor cells relative to wild type, with total cycle times significantly longer than previously reported periods associated with the native state (Table 2; Solon *et al.*, 2009). We speculate that the prolonged formation and dissolution times, in combination with the directed myosin observed in the nearest neighbors, lead to the dampened oscillations observed. Thus the expanded and constricted states of a cell induced, respectively, by Rho inactivation and activation can cell autonomously and nonautonomously influence myosin organization and dynamics in space and time. The additional dampening observed in RhoV14 distant neighbors may result from the nonautonomous influence of the epidermis and/or the AS–epidermis interface due to the epidermal expression also driven by the Gal4, analogous to the previously reported influence of zippering on pulsed constrictions (Jacinto *et al.*, 2002; Solon *et al.*, 2009).

In addition to influencing cytoskeletal organization, Rho GTPases regulate cell adhesion mediated by cadherins (Braga *et al.*, 1997). It is therefore possible that the effects on cytoskeletal dynamics we observe are secondary to effects on cell adhesion. Indeed, studies have revealed the influence of adhesion heterogeneities on myosin dynamics (Rauzi *et al.*, 2010). Alternatively, changes in adhesion may be a consequence of myosin dynamics. To resolve whether adhesion

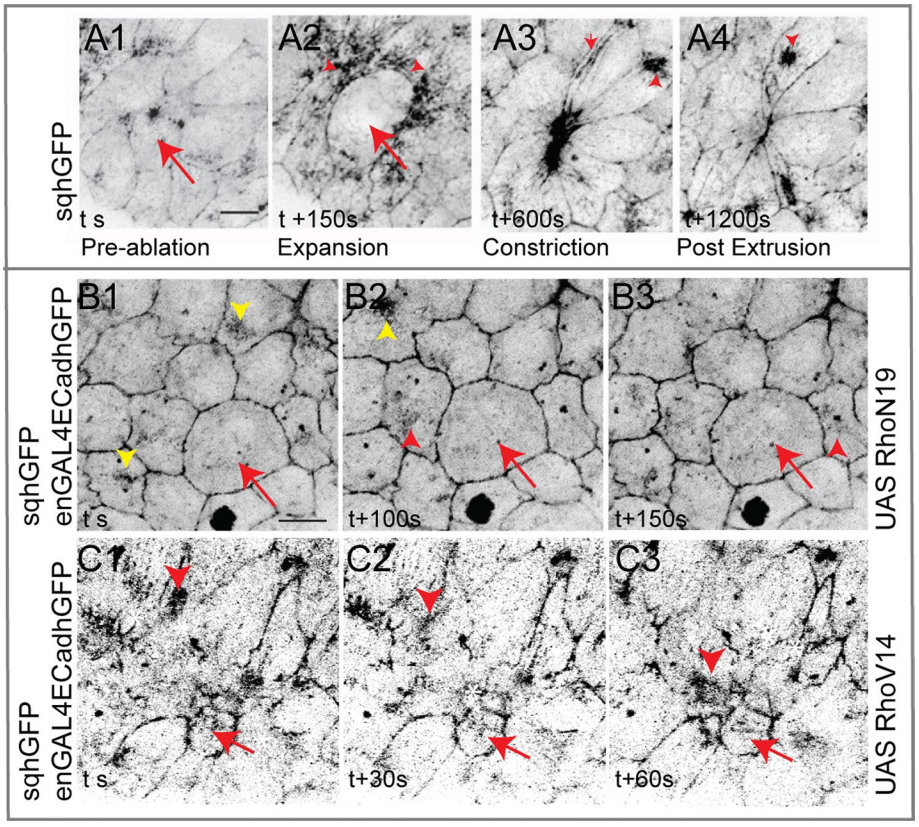

FIGURE 5: Effect of single-cell genetic and mechanical perturbations on the cytoskeleton. Myosin dynamics in and around a laser-perturbed cell (red arrows in A1–A4), a RhoN19-expressing cell (B1–B3) or RhoV14-expressing cell (C1–C3; red arrows in B, C), and their NeNe (red arrowheads) or DiNe (yellow arrowheads in B1–B3). Scale bar, 10 µm. See Supplemental Figure S5 for supporting data.

defects are a cause or consequence of cell-shape changes observed, we determined when, in relation to changes in cell geometry, adhesion defects are manifest. For this, we quantified cell geometries using a cell constriction index (CI; see *Materials and Methods*; CI > 1 indicates expansion, and CI < 1 indicates constriction) and determined in each case whether adhesion defects were evident before overt changes in cell morphology (CI = 1). Using these criteria, we analyzed 11 unexpanded (CI < 1.5) and 17 expanded (CI > 1.5) Rho N19–expressing cells (from 14 embryos) and 16 constricted (CI < 0.5) and seven nonconstricted (CI > 0.5) Rho V14-expressing cells (from 12 embryos).

Breaks in the continuity of cadherin immunoreactivity and apparent thinning were found in the membranes surrounding the single expanded RhoN19 cells (in 17 of 17 cells). In perturbed cells that were not (yet) expanded (11 of 11), cadherin staining looked largely normal (Supplemental Figure S5, A, A′, B, and B′). In addition, whereas enrichment of E-cadherin was found around membranes of single constricted RhoV14 cells (15 of 16 cells), no changes in adhesion were detected in nonconstricted RhoV14 cells (seven of seven cells; Supplemental Figure S5, A, A′, C, and C′). Importantly, no global differences in E-cadherin intensity or localization in the rest of the AS was observed in either perturbation. These results allow us to suggest that defects in cadherin localization may follow cell-shape defects rather than precede it and that the effects on local cell geometry must underlie the influence of Rho1 on cytoskeletal organization and cell adhesion.

The similarity of the influences of Rho1 and mechanical perturbations in single cells on pulsed behavior and myosin dynamics in the nearest neighbors prompts the suggestion that autonomous and nonautonomous changes in myosin reorganization induced by changes in tension and geometry may underlie the effects of both.

Myosin dynamics influences transitions from pulsed to unpulsed cell behavior nonautonomously

To establish that nonautonomous changes in myosin dynamics mediate the responses to changing tensions and geometries induced by Rho GTPases and mechanical perturbations, we examined the response to mechanical stress upon perturbing myosin. For this, we performed laser ablation on embryos expressing myoII^{DN}. We exploited the patchiness of the amnioserosa-specific Gal4 to independently deliver a mechanical stress to amnioserosa cells expressing or not expressing myoII^{DN}.

Cells expressing myoII^{DN} failed to respond normally to the ablation, evident from their inability to expand, constrict, and delaminate (in four of five cells from five embryos; Figure 6, A and B, and Supplemental Movie S7). Whereas the failure of expansion suggests that contractile myosin complexes are necessary for the maintenance of internal tension and through it, the prestressed state, the failure of constriction and delamination may be a consequence of perturbing myosin dynamics in neighboring cells. Indeed, only very small changes in shapes or areas were observed over a period of 10 min not only in the perturbed cell, but also in its neighbors (Figure 6, B1–B6). This suggests that myosin-dependent contractility is also necessary to generate significant changes in cell geometry. To test the possibility that myosin dynamics dictates the response to changes in cell geometry, we examined the response to ablation of

	Dynamics		Asynchrony	
Wt	3.9 (n = 5)		3.5 (n = 5)	
RhoN19	NeNe	DiNe	NeNe	DiNe
	2.3* (n = 16)	3.4 (n = 10)	3.0** (n = 16)	4.3 (n = 10)

N = 4 embryos. Values are mean deviations. *p = 0.03; **p = 0.005.

TABLE 1: Asynchrony and dynamics in myosin in RhoN19 cohorts.

	Formation (s)		Dissolution (s)	
Wt	65.4 ± 14 (n = 8)		39.6 ± 8 (n = 8)	
RhoV14	NeNe	DiNe	NeNe	DiNe
	116.1 ± 36.5* (n = 7)	133.6 ± 47* (n = 8)	235 ± 73* (n = 7)	200.4 ± 57.4* (n = 8)

N = 3 embryos. Errors are SD. *p < 0.0001.

TABLE 2: Myosin cycle times in RhoV14 cohorts.

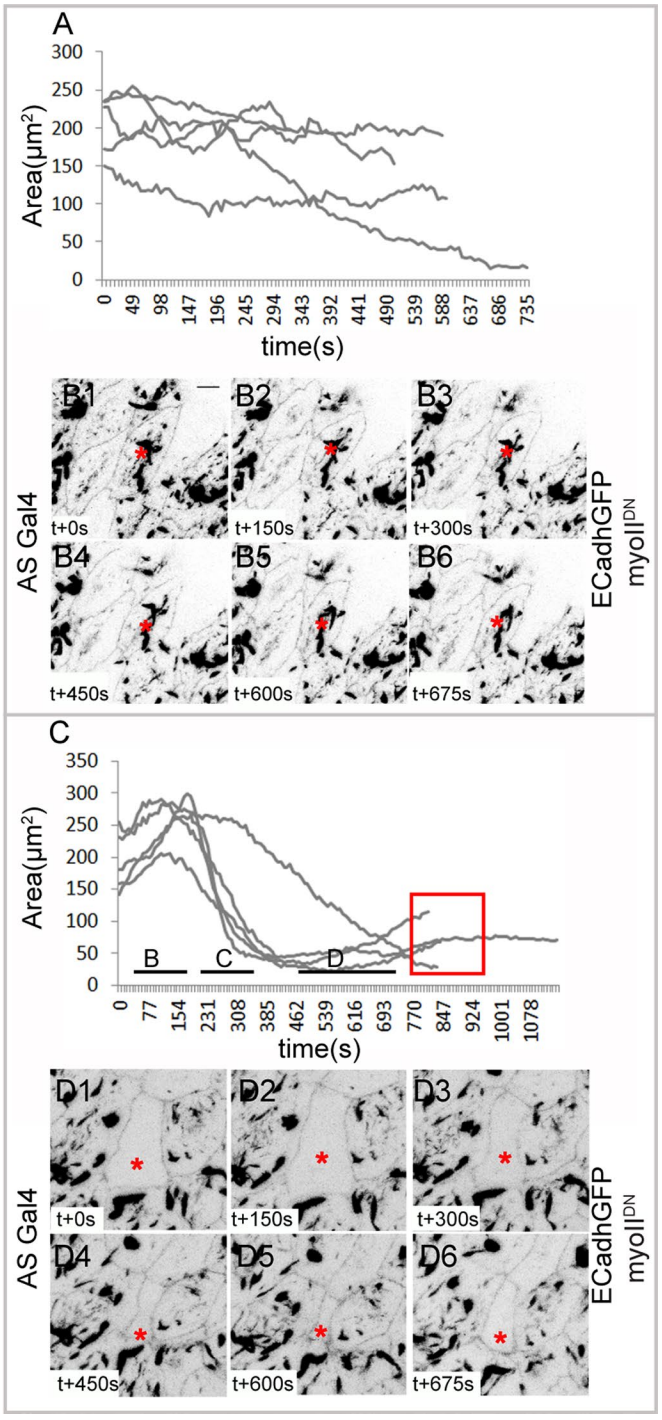

FIGURE 6: Autonomous and nonautonomous membrane and myosin dynamics in response to laser perturbation in contraction-defective cells. (A) Apical area curves of cells expressing myoII^{DN} ($n = 5$ from five embryos) and their membrane dynamics (B1–B6) upon laser perturbation. (C) Apical area curves of nonexpressing cells surrounded by cells expressing myoII^{DN} ($n = 5$ from five embryos) and their membrane dynamics (D1–D6) upon laser perturbation. Red box in C shows increase in area and failure of extrusion. Asterisks indicate the laser-perturbed cell. Scale bar, 10 μm.

nonexpressing cells surrounded by myo II^{DN}-expressing neighbors. Such a perturbation resulted in expansion of the perturbed cell followed by constriction. However, the constriction did not culminate in extrusion, with the cell instead exhibiting contraction and relaxation phases and a gradual increase in cell area in phase D (in four of five cells from five embryos; Figure 6C). The examination of myoII^{DN} dynamics in the nearest neighbors revealed little or no reorganization: although some directed motion of small streaks of myo II^{DN} was occasionally observed, no evidence of coalesced structures directed toward the interface was ever observed. Further, no enrichment at the interfaces between the ablated cell and its nearest neighbor or shape changes characteristic of the nearest-neighbor response to ablation previously observed in wild-type embryos was evident (Figure 6, D1–D6, and Supplemental Movie S8; Meghana *et al.*, 2011). These observations demonstrate that 1) a contractile myosin pool in the nearest neighbors that can be directed is necessary to ensure contraction without intervening relaxation phases in the perturbed cell (as seen in the failure of the wild-type ablated cell surrounded by contraction-defective neighbors to sustain constriction, despite its ability to expand) and 2) myosin contractility acting cell autonomously is critical to the generation of cell geometries and internal tension that then induce nonautonomous changes in myosin dynamics and cell shapes (as seen in the failure to elicit dynamic shape changes in a contraction-defective cell or its neighbors in response to ablation).

Natural delamination is a locally patterned transition from pulsed to unpulsed constriction

Our analysis of mechanical and genetic perturbations showed that pulsation dampening in the nearest-neighbor cells is associated with either less motile (meshwork/noncoalescent and nonmotile) or polarized motile medial myosin complexes (rather than randomly directed myosin flows) or changes in the cycle period of medial myosin. Changes in myosin dynamics associated with changes in cell geometry (constriction of the delaminating cell and stretch of the nearest neighbors) also accompany natural cell delamination during native closure. During natural delamination, single cells (DC) exhibiting normal pulsed constrictions abruptly and stochastically begin to constrict without intervening relaxation phases and leave the epithelium. Thus delamination presents a native situation morphologically analogous to the constriction phases induced by mechanical perturbation or RhoV14 expression and culminates in cell extrusion. This raises the possibility that transitions occurring during native closure may also be triggered by changes in cell tension and geometry. We examined the apical area dynamics of delaminating cell cohorts in phase I. The delaminating cell exhibited no pulsations during its constriction, like the RhoV14-expressing cell and the constriction phase of the mechanically perturbed cell (Figure 7A). Alterations in myosin dynamics were evident in both the delaminating cell and its nearest neighbors. In the delaminating cell, medial myosin distribution was more homogeneous at the apical end of the cell and was progressively found to have a punctate distribution throughout the cell (Figure 7, C1–C2). In the nearest neighbors, on the other hand, myosin flows were directed toward the DC as its constriction progressed (Figure 7, B1–B3, and Supplemental Movie S9; Meghana *et al.*, 2011). Given these similarities, we examined the cell area dynamics of the nearest neighbors. Pulse amplitudes in the nearest neighbors of delaminating cells were assessed in both E-cadherin–GFP (ECadhGFP) embryos (Supplemental Figure S6) and embryos carrying both sqhGFP and ECadhGFP (Supplemental Figure S7), which facilitated the visualization of both membrane and myosin dynamics. Transient pulse dampening was detectable in the area dynamics of 20 of 23 nearest neighbors from eight cohorts containing a delaminating cell in sqhGFP/ECadhGFP embryos and in six of nine nearest neighbors in three cohorts from ECadhGFP embryos (Figure 7A and Supplemental Figures S6 and S7). Dampening was invariably observed during the constriction phase, although its time of onset

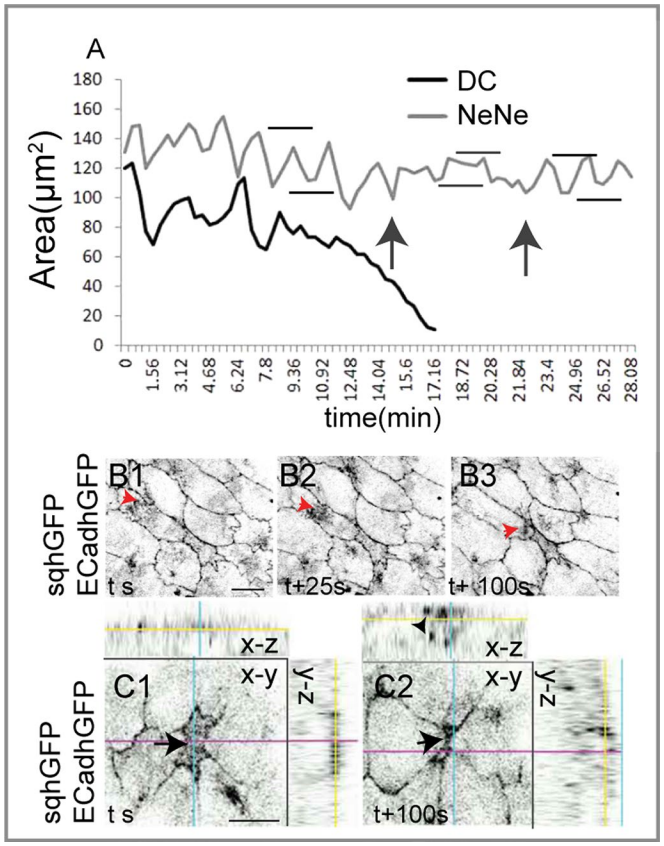

FIGURE 7: Autonomous and nonautonomous membrane and myosin response in naturally delaminating cells. (A) Representative apical area dynamics of one naturally delaminating cell (black curve) and a NeNe (gray curve) showing pulse dampening (gray horizontal bars denote amplitude, and black arrows denote duration) during constriction or extrusion of the delaminating cell. Black horizontal bars show A_{max} and A_{min} before cell constriction or upon recovery from dampening. (B1–B3) Membrane (ECadh GFP) and myosin (sqhGFP) dynamics in the NeNe (red arrowheads) directed toward the delaminating cell. (C1, C2) Time-lapse images of a naturally delaminating cell showing the apical (arrow) and basal (arrowhead) myosin pools. Scale bar, 10 μm. See Supplemental Figures S6 and S7 for further examples.

relative to the time of initiation of constriction in the DC was variable. On average, pulsations were dampened for 6.8 ± 1.4 min (n = 23). In all cases, pulsations reappeared, albeit at lower amplitudes, as the cell was extruded from the epithelium, similar to the pulsation dynamics observed in the mechanically perturbed cell and its nearest neighbors (Figure 7A and Supplemental Figures S6 and S7). This suggests that geometry and tension may also govern the nonautonomous regulation of pulse amplitude and myosin dynamics during natural delamination that occurs during native closure. We argue that the greater degree of anisotropy in shape and tension associated with natural delamination may contribute to the heterogeneity in the behavior of the nearest neighbors.

DISCUSSION

In this work, we set out to understand the nature and spatial origin of cues that account for the apparently asynchronous pattern of pulsed constrictions in the amnioserosa by perturbing single cells genetically (alterations in RhoGTPase or myosin activity) or biophysically (nanoscale laser ablation of cytoskeletal structures). The results provide for the first time a single-cell-resolution analysis of the regulation and spatiotemporal propagation of pulsed constrictions in an epithelium and their reliance on the organization and dynamics of medial myosin–containing complexes and provide several new insights. First, they establish for the first time that pulsed cell behavior can be influenced (genetically speaking) both cell-autonomously and -nonautonomously. Such nonautonomous effects are, from a geneticist's perspective, traditionally attributed to secreted molecules. Our results reveal, however, that this nonautonomy has a physical basis that can be attributed to the transmission of tension between adjacent cells. Indeed, in a sheet composed of mechanically connected cells, as all tissues are, it is both intuitive and imperative to expect nonautonomous influences. The influences common to laser ablation, defective myosin contractility, or altered RhoGTPase activity and natural delamination allow us to 1) strongly argue that local modulation of tension and/or geometry indeed underlie their cell-autonomous and -nonautonomous influences on the spatial pattern and propagation of pulsed constrictions and 2) visualize the range of this influence and uncover its dependence on the nature of the perturbation. They further demonstrate that changes in tension and geometry thus induced provide cues for myosin organization and dynamics. Finally, they establish that the regulation of myosin dynamics (quality, amplitude, direction) underlies the (autonomous and nonautonomous) influence of these cues. Collectively, they 1) argue that changes in cell tension and geometry may underlie the effects of both perturbations and 2) suggest the existence of a feedback mechanism that regulates the emergence of patterned cell behavior in a tissue in response to dynamic changes in stretch/tension during morphogenesis (Figure 8).

The importance of tension and geometry in driving transitions in cell behavior

The features common to both mechanical and genetic perturbations allow us to suggest that differences in the nature of stresses and the changes in geometry they induce must underlie the influences of both (Figure 8, A–D). Our experiments with myo II^{DN} also establish the necessity of cytoskeletal contractility in generating, sensing, and responding to stresses. They thus uncover the interplay between signals, internal stresses (myosin-dependent contractility), and external stresses in the patterning of cell behavior. Thus external stresses resulting from or as a response to changes in nearest-neighbor tension and geometry can influence internal stresses through myosin dynamics, which in turn can influence cell behavior both autonomously and nonautonomously through mechanical connectivity. This interplay, we suggest, enables an adaptive feedback mechanism by which to trigger transitions in cell behavior and spatially propagate pattern in tissues. We suggest that myosin-dependent contractility helps to maintain connectivity of the actin cytoskeleton and through it enables it to sense and adjust tensions in a sheet of cells. Such a role is in line with the model of Sheetz and colleagues, who demonstrated the need for myosin II–dependent cytoskeletal coherence during cell spreading (Cai *et al.*, 2010). In this respect, the epithelium we study here (the amnioserosa) is similar to smooth muscle (where stretch dependent regulation of contractility was first documented) and also to the single-celled *Caenorhabditis elegans* embryo, in which anisotropies in tension generated by asymmetries in the actomyosin network influence cytoskeletal dynamics (Munro *et al.*, 2004; Mayer *et al.*, 2010; Stewart *et al.*, 2011).

Our results also suggest that cell adhesion defects downstream of Rho1 and mechanical stress may be consequences of changes in geometry and tension rather than their cause. Our experiments, however, do not rule out the possibility that adhesion defects

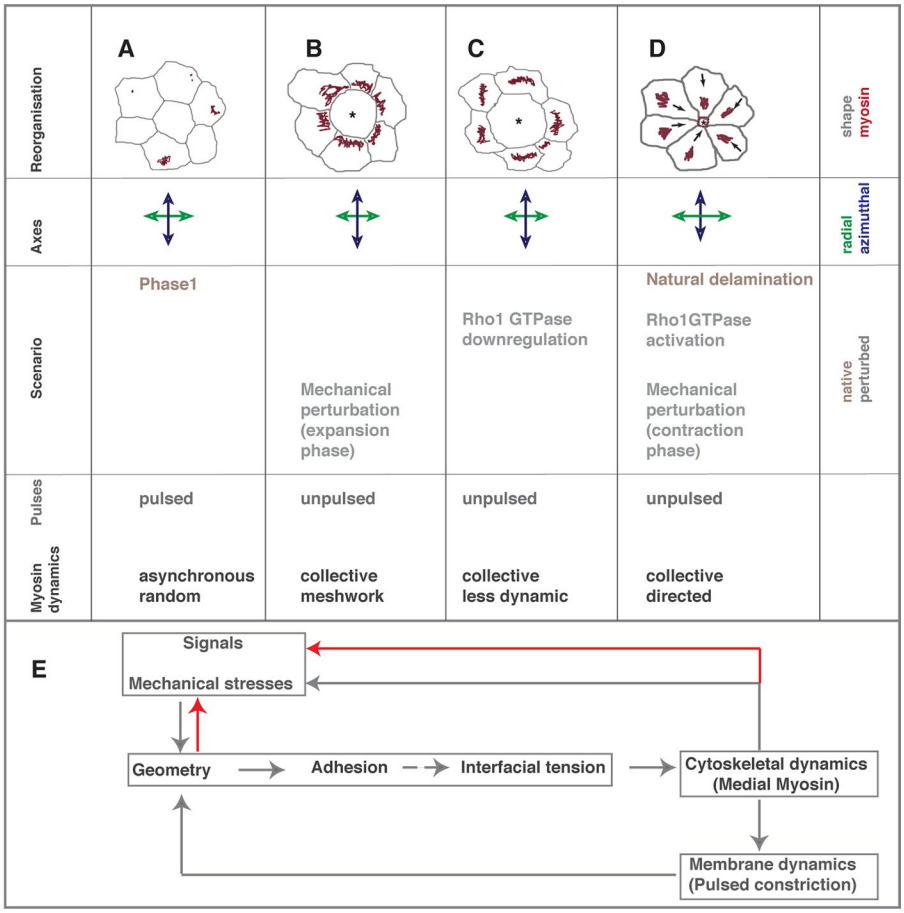

FIGURE 8: Controls on myosin dynamics and transitions in cell behavior. (A–D) The autonomous and nonautonomous effects of single-cell (asterisk) mechanical and genetic perturbations or stochastically occurring natural delamination on local pattern and cell shape (gray, top), myosin dynamics (red, top, direction indicated by arrows), deformation of radial (green) and azimuthal (blue) axes, and cell area fluctuations. (E) The feedback loop uncovered by this study. Solid gray arrows represent hierarchies proven by this study, and stippled arrows indicate presumed hierarchies. Interactions uncovered by other studies are indicated by red arrows.

precede shape changes by a time interval smaller than what our study is able to resolve. Thus we propose that dynamic geometries influence interfacial tension through adhesion to direct cytoskeletal organization and pulsation dynamics. The latter in turn may influence geometry and also activate Rho1, thus forming a feedback loop (Figure 8E). It is plausible that differences in the magnitude of stress also contribute to the differences in cell behavior, as borne out in the qualitative differences in the myosin response to cell expansion induced mechanically and genetically.

The applicability of the results obtained from perturbations extends to naturally occurring transitions in cell behavior and allow us to argue that cell delamination (Meghana *et al.*, 2011) ensues when stresses act isotropically on a single cell through collectivity in the nearest neighbors or from loss of prestress within the delaminating cell. Although this collectivity may be a chance happening in a dynamic tissue, our results suggest that its emergence may be a consequence of stress perturbations in a single cell.

Although seemingly intuitive as suggested, our evidence for local, nonautonomous regulation differs from the observations of He *et al.* (2010), which documented purely cell-autonomous regulation of pulsed constrictions, albeit in a different tissue. We speculate that this difference may arise from differences in the dynamics of cells in the two tissues and consequently in the origin and nature of dynamic stresses and geometries encountered by cells in the two cases.

We have loosely used the word asynchrony to describe the observation that membrane and cytoskeletal cycles that characterize pulsed cell behavior are not in phase in adjacent cells. What is borne out from our work is that this out-of-phase behavior is the manifestation of the influence of one cell's behavior on the state of its neighbors to which cells appear to be constantly tuned. We speculate that underneath the seeming asynchrony must lie a hidden (temporal) order dictated by the pattern of stress propagation. Visualizing the correlative dynamics of stresses, signal states, and cytoskeleton will enable the delineation of their spatial and temporal hierarchies.

The importance of directing myosin dynamics

Our results establish that pulse dampening is mediated by reorganization of myosin dynamics. This can be accomplished by 1) the absence of contractile actomyosin complexes (in the mechanically perturbed/RhoN19/myoII^{DN}-expressing cell), 2) changes in their organization (stable meshworks rather than motile complexes in the transition from phase I to phase II of dorsal closure, diffuse complexes in Rho N19 nearest neighbors, and meshworks in the early response of nearest neighbors of a mechanically perturbed cell in myoII^{DN}-expressing cells), and 3) changes in their mobility in space and in time (by influencing cycle length [Rho V14 NeNe], myosin flow direction [NeNe of RhoN19, RhoV14, late response to mechanical perturbation, and in naturally delaminating cells]). Polarized flows of myosin are also observed in the *C. elegans* zygote, where they are initiated by asymmetries in tension/pressure (sperm entry–induced destabilization of the actomyosin network, hydrostatic pressure; Munro *et al.*, 2004; Stewart *et al.*, 2011). These flows aid the asymmetric localization of polarity determinants, critical not only for the subsequent axial patterning of the embryo, but also for the feedback regulation of the actomyosin network. Whether directed myosin flows we observe in the nearest neighbors also generate asymmetries in protein localization in the nearest neighbors remains to be determined.

The molecular mechanisms that lead to differences in myosin organization remain to be understood. Spatially regulated myosin dynamics has been shown to be both triggered by and responsible for the generation of differences in adhesion cell autonomously during cell intercalation (Rauzi *et al.*, 2010; Levayer *et al.*, 2011), the latter occurring downstream of RhoGEF2. Our earlier work demonstrated that some features of myosin organization in response to mechanical stress rely on an intact microtubule cytoskeleton (Meghana *et al.*, 2011), which becomes polarized in response to it. It is therefore likely that the spatial propagation of pulsed constrictions must also rely on the dynamic cross-talk between the actomyosin and microtubule cytoskeleton.

Mechanochemical hierarchies underlying oscillatory cell behavior and myosin dynamics

Our results uncover striking similarities in the influence of mechanical and genetic perturbations both autonomously and nonautonomously: Rho inactivation recapitulated the effect of cell expansion/loss of cellular prestress, whereas its constitutive activation mimicked the effects of cell constriction/increased cortical tension. Of importance, both influence and lock the conformations of the cell and its neighbors, and neither culminates in delamination. This suggests that GTPase cycling may be an integral component of the dynamic response to mechanical stresses. Our results, however, do not allow us to delineate the hierarchy of mechanics and chemistry. Although they demonstrate that Rho activation and inactivation can, through autonomous effects on tension/cell shape, that is, expansion and constriction, influence stresses nonautonomously, its cycle may in turn be influenced by stresses. Rho activation and relocalization were demonstrated to occur around gaping wound edges (Clark *et al.*, 2009), which we suspect must be mechanically triggered (Meghana *et al.*, 2011), and the periodicity of their cycle is also consistent with the protrusion–retraction cycle of a moving lamellipod (Tkachenko *et al.*, 2011). Indeed, work published while our manuscript was under revision (Burkel *et al.*, 2012) suggests that RhoGTPase signals may also treadmill in response to internal/external stress.

On the origin of pulsed cell behavior in the amnioserosa

Our results also help to reconcile two conflicting reports on the origin of pulsed behavior in the amnioserosa (reviewed in Kasza and Zallen, 2011; Lecuit *et al.*, 2011) by demonstrating that it can be regulated both locally (intrinsic to the AS, as also reported in Blanchard *et al.*, 2010, but acting both cell autonomously and nonautonomously, as we discuss here) and at a distance (as described in Solon *et al.*, 2009, and as we observe in the case of RhoV14). Both, we argue, rely on mechanical influences originating at different distances and differing in their magnitude and scale of influence.

In conclusion, the results we report here allow us to infer the rules of interaction between cells in the spatial patterning of tissues (Figure 8E) and highlight the importance of cell-nonautonomous influences of tension and geometry acting locally to feedback control cell behavior. They establish seminal roles for the organization of myosin dependent contractility in generating, sensing, and responding to changing tensions and geometries and provide the basis for a feedback mechanism that relies on the interplay between stresses, signals, and geometry that is both sensitive and adaptive. Our results also provide experimental support for a theoretical cell-level biomechanical model for sustained area oscillations in the amnioserosa that invokes the "coupling between myosin dynamics, mechanical deformation and signals" published while our manuscript was being revised (Wang *et al.*, 2013).

MATERIALS AND METHODS

Drosophila stocks

The following stocks were used: UbiE-CadherinGFP (a kind gift of Tadashi Uemura [Kyoto University, Japan]; Uemura *et al.*, 1996) to label the apical membrane; sqhGFP in otherwise wild-type or sqh^{AX3} mutant background to monitor myosin dynamics (a kind gift from J. Raff [Oxford University, UK], Talila Volk [Weizmann Institute, Israel], and A. Saxena [Cambridge University, UK]; Royou *et al.*, 2004); UAS YFP $myoII^{DN}$ to perturb myosin contractility (a kind gift of Andrea Brand [Gurdon Institute, Cambridge, UK]; Dawes-Hoang *et al.*, 2005); UAS Actin5CGFP to visualize actin dynamics; engrailedGal4 (enGal4; to drive expression in single cells); c381Gal4 (AS Gal4, to drive expression in AS cells); and UAS RhoN19 and UAS V14 to down-regulate and constitutively activate RhoA and UAS GFP to label perturbed cells (all from Bloomington *Drosophila* Stock Center, Indiana University, Bloomington, IN). A stable UAS RhoV14 sqh GFP recombinant was made (this study) to visualize the effect of Rho activation on myosin dynamics.

A full list of genotypes analyzed is as follows. The genotype of the first chromosome is *w* unless otherwise stated.

For live imaging

w; ECadhGFP: to visualize membrane deformations and measure areas in the native state and in response to laser ablation.

w; sqhGFP and *y w* sqh^{AX3}; sqhGFP: to visualize myosin dynamics.

w; ECadhGFP/sqhGFP: to visualize membrane and myosin responses simultaneously.

w; ECadhGFP/+; UAS YFP $myoII^{DN}$/+; c381Gal4/+: to perturb contractility and visualize membrane and $myoII^{DN}$ dynamics natively and in response to mechanical perturbation.

w; ECadhGFP/+;; c381Gal4/+: to visualize membrane dynamics in cells with a single copy of AS Gal4.

w; enGAL4 ECadhGFP/+; UASActin5CGFP/+: as a control for single-cell (labeled with actin GFP) perturbations.

w; enGAL4 ECadhGFP/+; UAS Actin5CGFP/UAS RhoN19: to visualize membrane responses to genetically induced cell expansion through single-cell perturbations (labeled with actin GFP) of RhoA (down-regulation).

w; enGAL4 ECadhGFP/sqhGFP; UAS RhoN19/+: to visualize myosin and membrane responses to genetically induced cell expansion through single-cell perturbations of RhoA (down-regulation).

w; enGAL4 ECadhGFP/UAS RhoV14; UAS Actin5CGFP/+: to visualize membrane responses to genetically induced cell constriction through single-cell perturbations (labeled with actin GFP) of RhoA (constitutive activation).

w; enGAL4 ECadhGFP/UAS RhoV14 sqhGFP: to visualize myosin and membrane responses to genetically induced cell constriction through single-cell perturbations of RhoA (constitutive activation).

For fixed preparations

w;; UAS YFP $myoII^{DN}$/+; c381Gal4/+: to visualize $myoII^{DN}$ and pMLC

w; enUASGFP/+; UASRhoN19/+: to visualize adhesion and cytoskeleton in Rho down-regulated cells.

w; enUASGFP/UASRhoV14: to visualize adhesion and cytoskeleton in Rho up-regulated cells.

Cell tracking and data analysis

The absolute apical cell area was extracted manually from maximum-intensity projections of apical confocal slices using ImageJ (National Institutes of Health, Bethesda, MD). Normalized areas were calculated as A_t/A_0. The normalized fluctuations were calculated as $A_t - A_{t+1}/A_t$. Normalized pulse amplitudes were calculated as $(A_{max}/A_0) - (A_{min}/A_0)$, where A_{max} and A_{min} represent, respectively, the maximum and minimum apical cell areas during a pulse and A_0 denotes the initial cell area. Pulse amplitudes were calculated from all pulses over a period of 30 min from single perturbed cells in phase I and then averaged over several embryos to obtain mean amplitudes and deviations. Statistical parameters were computed and graphs plotted using Excel 2007 (Microsoft, Redmond, WA). Unpaired *t* test was used to assess significance of differences between means using Instat

(GraphPad Software, La Jolla, CA). The constricted and expanded states of the cell were assessed using the cell constriction index, CI, calculated as area of the expressing cell/average of the cell areas of the nearest neighbors (Muliyil *et al.*, 2011). The criteria for constricted and expanded states were fixed as CI ≤ 0.5 and ≥ 1.5, respectively.

Antibodies and live imaging

Egg laying was allowed for 4.5–6 h and aging of the embryos for 8.5–5.5 h, respectively, to enrich stage 13–14 embryos. All the experiments were done at 25°C except for the myoII^{DN} experiments, which were done at 29°C. The following primary antibodies were used: anti-GFP (rabbit, 1:1000 [Invitrogen, Carlsbad, CA] and mouse, 1:50 [Bangalore Genei Bangalore, India]), anti–E-cadherin (1:10; Development Studies Hybridoma Bank, University of Iowa, Iowa City, IA), and anti-pMLC (1:50; Cell Signaling Technology, Beverly, MA). Fluorophore-conjugated secondary antibodies and rhodamine–phalloidin (Invitrogen) were used at 1: 200 dilution. Embryos were stained using standard protocols (Narasimha and Brown, 2006).

For live imaging, stage 13 *Drosophila* embryos were imaged using a Zeiss 710 Meta Microscope (Carl Zeiss, Jena, Germany) and a Plan-Neofluar 63× oil immersion (1.4 numerical aperture) objective. Optical sections 0.3/1 µm apart (for fixed/live), covering the thickness of the amnioserosa cells, were captured, yielding a temporal resolution of two to four three-dimensional frames/min. Maximum-intensity projections at each time were assembled to make the time series using ImageJ, and figures were composed using Photoshop and Illustrator (Adobe, San Jose, CA).

Quantitative analysis of myosin dynamics

Medial myosin intensities were determined as the mean fluorescence intensity within a cytoplasm-encompassing region of interest. For the estimation of spatial (a)synchrony in myosin organization within a cohort of NeNe cells, the deviation in intensity from the mean was computed for each cohort over a period of 30 min. Multiple cohorts were measured and the average deviation computed (see Eqs. 1 and 2). For the estimation of medial myosin dynamics, the deviation in intensity in a given NeNe cell over a period of 30 min was measured. The deviations obtained from the analysis of several NN cells across a similar period were then averaged (see Eqs. 3 and 4). For the estimation of the length of the myosin cycle, the time to formation (attainment of largest size from the size of its initial detection) and the time to dissolution (attainment of largest size to its complete disappearance) was determined for multiple NeNe and DiNe cells and averaged. The total cycle time was calculated as the sum of the two times and does not include a potential lag period between two cycles. The significance of differences between means was calculated using GraphPad software.

Spatial asynchrony

$$\mathrm{Std}_{t1} = \sqrt{1/N \sum_{i=1}^{N} \left(MI_i - \overline{MI}\right)} \quad (1)$$

where *MI* is the myosin intensity and *N* is the number of NeNe cells.

$$\mathrm{Asynchrony} = \frac{\sum_{x=1}^{N} \mathrm{Std}_{tx}}{N} \quad (2)$$

where *N* is the time (30 min).

Medial myosin dynamics

$$\mathrm{Std} = \sqrt{1/N \sum_{i=1}^{N} \left(MI_i - \overline{MI}\right)} \quad (3)$$

where *N* is the time (30 min).

$$\mathrm{Dynamics} = \frac{\sum_{x=1}^{N} \mathrm{Std}_{tx}}{N} \quad (4)$$

where *N* is the number of NeNe cells.

Subcellular laser perturbations

To mechanically expand and compress cells, single amnioserosa cells were subject to subcellular laser perturbations using a pulsed titanium sapphire laser system as previously described (Meghana *et al.*, 2011), without perturbing the integrity of the membrane. All the ablations were of the size of a diffraction-limited spot in the cytoplasm, 2 µm below the apical plasma membrane, and performed on single cells located in the center of the AS and during phase I of dorsal closure. They were imaged to capture pulsations before, during, and after ablation.

ACKNOWLEDGMENTS

We thank Andrea Brand, Roger Karess, Jordan Raff, A. Saxena, Tadashi Uemura, the Bloomington *Drosophila* Stock Center, and Priyamvada Chugh for fly stocks; the Development Studies Hybridoma Bank for antibodies; members of the Narasimha lab and Srikanth Sastry and Roddam Narasimha for discussions; reviewer 2 for insightful and constructive comments on the manuscript; colleagues at the Department of Biological Sciences for support; and the Tata Institute of Fundamental Research for funding (to M.N.).

REFERENCES

Bershadsky AD, Ballestrem C, Carramusa L, Zilberman Y, Gilquin B, Khochbin S, Alexandrova AY, Verkhovsky AB, Shemesh T, Kozlov MM (2006). Assembly and mechanosensory function of focal adhesions: experiments and models. Eur J Cell Biol 85, 165–173.

Blanchard GB, Murugesu S, Adams RJ, Martinez-Arias A, Gorfinkiel N (2010). Cytoskeletal dynamics and supracellular organisation of cell shape fluctuations during dorsal closure. Development 137, 2743–2752.

Bloor JW, Kiehart DP (2002). Drosophila RhoA regulates the cytoskeleton and cell-cell adhesion in the developing epidermis. Development 129, 3173–3183.

Braga VM, Machesky LM, Hall A, Hotchin NA (1997). The small GTPases Rho and Rac are required for the establishment of cadherin-dependent cell-cell contacts. J Cell Biol 137, 1421–1431.

Burkel BM, Benink HA, Vaughan EM, von Dassow G, Bement WM (2012). A Rho GTPase signal treadmill backs a contractile array. Dev Cell 23, 384–396.

Cai Y, Rossier O, Gauthier NC, Biais N, Fardin MA, Zhang X, Miller LW, Ladoux B, Cornish VW, Sheetz MP (2010). Cytoskeletal coherence requires myosin-IIA contractility. J Cell Sci 123, 413–423.

Clark AG, Miller AL, Vaughan E, Yu HY, Penkert R, Bement WM (2009). Integration of single and multicellular wound responses. Curr Biol 19, 1389–1395.

David DJ, Tishkina A, Harris TJ (2010). The PAR complex regulates pulsed actomyosin contractions during amnioserosa apical constriction in *Drosophila*. Development 137, 1645–1655.

Dawes-Hoang RE, Parmar KM, Christiansen AE, Phelps CB, Brand AH, Wieschaus EF (2005). Folded gastrulation, cell shape change and the control of myosin localization. Development 132, 4165–4178.

Gorfinkiel N, Blanchard GB, Adams RJ, Martinez Arias A (2009). Mechanical control of global cell behaviour during dorsal closure in *Drosophila*. Development 136, 1889–1898.

He L, Wang X, Tang HL, Montell DJ (2010). Tissue elongation requires oscillating contractions of a basal actomyosin network. Nat Cell Biol 12, 1133–1142.

Jacinto A, Wood W, Woolner S, Hiley C, Turner L, Wilson C, Martinez-Arias A, Martin P (2002). Dynamic analysis of actin cable function during *Drosophila* dorsal closure. Curr Biol 12, 1245–1250.

Jaffe AB, Hall A (2005). Rho GTPases: biochemistry and biology. Annu Rev Cell Dev Biol 21, 247–269.

Kasza KE, Zallen JA (2011). Dynamics and regulation of contractile actin-myosin networks in morphogenesis. Curr Opin Cell Biol 23, 30–38.

Kiehart DP, Galbraith CG, Edwards KA, Rickoll WL, Montague RA (2000). Multiple forces contribute to cell sheet morphogenesis for dorsal closure in *Drosophila*. J Cell Biol 149, 471–490.
Lecuit T, Le Goff L (2007). Orchestrating size and shape during morphogenesis. Nature 450, 189–192.
Lecuit T, Lenne PF, Munro E (2011). Force generation, transmission, and integration during cell and tissue morphogenesis. Annu Rev Cell Dev Biol 27, 157–184.
Levayer R, Pelissier-Monier A, Lecuit T (2011). Spatial regulation of Dia and myosin-II by RhoGEF2 controls initiation of E-cadherin endocytosis during epithelial morphogenesis. Nat Cell Biol 13, 529–540.
Martin AC, Gelbart M, Fernandez-Gonzalez R, Kaschube M, Wieschaus EF (2010). Integration of contractile forces during tissue invagination. J Cell Biol 188, 735–749.
Martin AC, Kaschube M, Wieschaus EF (2009). Pulsed contractions of an actin-myosin network drive apical constriction. Nature 457, 495–499.
Mayer M, Depken M, Bois JS, Julicher F, Grill SW (2010). Anisotropies in cortical tension reveal the physical basis of polarizing cortical flows. Nature 467, 617–621.
Meghana C, Ramdas N, Hameed FM, Rao M, Shivashankar GV, Narasimha M (2011). Integrin adhesion drives the emergent polarization of active cytoskeletal stresses to pattern cell delamination. Proc Natl Acad Sci USA 108, 9107–9112.
Muliyil S, Krishnakumar P, Narasimha M (2011). Spatial, temporal and molecular hierarchies in the link between death, delamination and dorsal closure. Development 138, 3043–3054.
Munro E, Nance J, Priess JR (2004). Cortical flows powered by asymmetrical contraction transport PAR proteins to establish and maintain anterior-posterior polarity in the early *C. elegans* embryo. Dev Cell 7, 413–424.
Narasimha M, Brown NH (2004). Novel functions for integrins in epithelial morphogenesis. Curr Biol 14, 381–385.
Narasimha M, Brown NH (2006). Confocal microscopy of *Drosophila* embryos. In: Cell Biology: A Laboratory Handbook, Vol. 3, ed. JE Celis, San Diego, CA: Academic Press, 77–86.
Rauzi M, Lenne PF, Lecuit T (2010). Planar polarized actomyosin contractile flows control epithelial junction remodelling. Nature 468, 1110–1114.
Royou A, Field C, Sisson JC, Sullivan W, Karess R (2004). Reassessing the role and dynamics of nonmuscle myosin II during furrow formation in early *Drosophila* embryos. Mol Biol Cell 15, 838–850.
Sawyer JM, Harrell JR, Shemer G, Sullivan-Brown J, Roh-Johnson M, Goldstein B (2009). Apical constriction: a cell shape change that can drive morphogenesis. Dev Biol 341, 5–19.
Solon J, Kaya-Copur A, Colombelli J, Brunner D (2009). Pulsed forces timed by a ratchet-like mechanism drive directed tissue movement during dorsal closure. Cell 137, 1331–1342.
Stewart MP, Helenius J, Toyoda Y, Ramanathan SP, Muller DJ, Hyman AA (2011). Hydrostatic pressure and the actomyosin cortex drive mitotic cell rounding. Nature 469, 226–230.
Tkachenko E, Sabouri-Ghomi M, Pertz O, Kim C, Gutierrez E, Machacek M, Groisman A, Danuser G, Ginsberg MH (2011). Protein kinase A governs a RhoA-RhoGDI protrusion-retraction pacemaker in migrating cells. Nat Cell Biol 13, 660–667.
Uemura T, Oda H, Kraut R, Hayashi S, Kotaoka Y, Takeichi M (1996). Zygotic *Drosophila* E-cadherin expression is required for processes of dynamic epithelial cell rearrangement in the *Drosophila* embryo. Genes Dev 10, 659–671.
Wang Q, Feng JJ, Pismen LM (2013). A cell-level biomechanical model of Drosophila dorsal closure. Biophys J 103, 2265–2274.
Watanabe N, Kato T, Fujita A, Ishizaki T, Narumiya S (1999). Cooperation between mDia1 and ROCK in Rho-induced actin reorganization. Nat Cell Biol 1, 136–143.